THE JOURNAL OF PHYSICAL CHEMISTRY Letters

Letter

pubs.acs.org/JPCL

Nuclear Quantum Effects in Water Reorientation and Hydrogen-Bond Dynamics

David M. Wilkins,[*,†] David E. Manolopoulos,[*,‡] Silvio Pipolo,[*,¶,∥,§] Damien Laage,[*,¶,∥] and James T. Hynes[*,¶,⊥]

[†]Laboratory of Computational Science and Modeling, IMX, École Polytechnique Fédérale de Lausanne, 1015 Lausanne, Switzerland

[‡]Physical and Theoretical Chemistry Laboratory, University of Oxford, South Parks Road, Oxford OX1 3QZ, United Kingdom

[¶]PASTEUR, Département de Chimie, École Normale Supérieure, UPMC Univ Paris 06, CNRS, PSL Research University, 75005 Paris, France

[∥]Sorbonne Universités, UPMC Univ Paris 06, ENS, CNRS, PASTEUR, 75005 Paris, France

[⊥]Department of Chemistry and Biochemistry, University of Colorado, Boulder, Colorado 80309-0215, United States

Supporting Information

ABSTRACT: We combine classical and ring polymer molecular dynamics simulations with the molecular jump model to provide a molecular description of the nuclear quantum effects (NQEs) on water reorientation and hydrogen-bond dynamics in liquid H_2O and D_2O. We show that while the net NQE is negligible in D_2O, it leads to a ∼13% acceleration in H_2O dynamics compared to a classical description. Large angular jumps—exchanging hydrogen-bond partners—are the dominant reorientation pathway (just as in a classical description); the faster reorientation dynamics arise from the increased jump rate constant. NQEs do not change the jump amplitude distribution, and no significant tunneling is found. The faster jump dynamics are quantitatively related to decreased structuring of the OO radial distribution function when NQEs are included. This is explained, via a jump model analysis, by competition between the effects of water's librational and OH stretch mode zero-point energies on the hydrogen-bond strength.

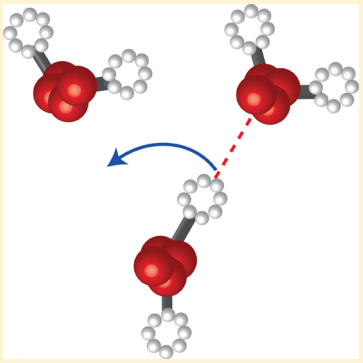

Water reorientation and hydrogen-bond (H-bond) network rearrangements are essential for a broad range of chemical and biochemical processes in aqueous solution, including proton transfer reactions, ion transport, protein folding, and ligand−biomolecule binding.[1−4] Because these water motions involve displacements of hydrogens with very small mass, an explicit description of quantum mechanical zero-point energy (ZPE) and tunneling effects may be necessary.[5,6] Indeed, recent simulations have established that competing nuclear quantum effects (NQEs) on the intra- and intermolecular interactions[7,8] lead to a net acceleration of water translational and rotational dynamics.[7,9−11] In the case of the rotational dynamics, it has been argued[12,13] on the basis of classical simulations that water reorientation proceeds via a mechanism involving sudden large angular jumps, in which H-bonding partners are exchanged during, in effect, a chemical reaction, a mechanism that is in strong contrast to the traditional Debye diffusion picture. If this jump mechanism also applies to quantum water, it could provide a detailed molecular picture of the factors responsible for the quantum rotational acceleration. But in fact, the relevance of the jump mechanism for water has been questioned, precisely because of the possible role of NQEs (see, e.g., refs 11 and 14).

Here we address these issues via classical molecular dynamics (MD) and, for the quantum case, thermostated ring polymer molecular dynamics (TRPMD)[15] simulations of H_2O and D_2O water reorientation and associated H-bond dynamics. We show that the molecular jump mechanism[12,13] remains valid when NQEs are included and that the dynamical acceleration induced by NQEs arises from faster H-bond jump exchanges within this mechanism. Finally, we establish that the isotope and NQEs on jump dynamics can be quantitatively inferred from the changes in the oxygen−oxygen radial distribution function (rdf).

All of our simulations employ the flexible q-TIP4P/F potential.[7] While more sophisticated potentials are now available (e.g., MB-pol[16]), they are more expensive to evaluate, and because q-TIP4P/F has been shown to reproduce the experimental structural and dynamical properties of liquid water when NQEs are included,[7] it is ideal for our present purposes. For both H_2O and D_2O, 216 water molecules are simulated at the experimental density[17] at 298 K and propagated in 50 independent 3 ns classical *NVE* runs and 20 independent 500 ps quantum TRPMD[15] trajectories.

The water reorientation dynamics are probed by the orientation time correlation functions

$$C_n(t) = \langle P_n[\mathbf{u}_{OH}(0)\cdot\mathbf{u}_{OH}(t)]\rangle \quad (1)$$

Received: April 21, 2017
Accepted: May 22, 2017
Published: May 22, 2017

DOI: 10.1021/acs.jpclett.7b00979
J. Phys. Chem. Lett. 2017, 8, 2602−2607

where $\mathbf{u}_{OH}(t)$ is the water OH (or OD) bond's orientation at time t and P_n is the nth-order Legendre polynomial (see the SI for their calculation within the RPMD approach). These are shown for $n = 1-3$ in Figure 1. Although only C_2 is experimentally accessible,[18] we also consider C_1 and C_3 because different orders have been suggested[7] to exhibit different NQEs. Following ref 13, we focus on reorientation beyond the initial subpicosecond librational decay and determine the reorientation times τ_n by an exponential fit of $C_n(t)$ to Ae^{-t/τ_n} for $4 \le t \le 15$ ps.

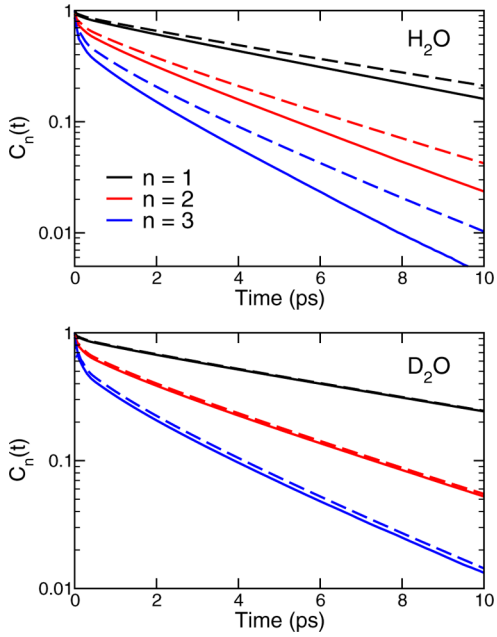

Figure 1. Orientation correlation functions $C_n(t)$ (eq 1) for $n = 1-3$ for H_2O (upper panel) and D_2O (lower panel), from classical MD (dashes) and TRPMD (solid lines) simulations.

In H_2O, Table 1's τ_n times show that, in agreement with previous studies,[7,9−11] NQEs accelerate water reorientational dynamics. An interesting feature is that the acceleration factor $\rho_n = \tau_n^{qm}/\tau_n^{cl}$ is independent of the order n of the orientational time correlation function and very similar to the value of 0.87 previously found[7] for the NQE on the translational dynamics of the same q-TIP4P/F model, suggesting a common origin for the NQE acceleration of rotational and translational dynamics. Our results further show that the increase of ρ_n with n found in ref 7 is actually caused by the subpicosecond librational (hindered rotational) water molecular motions and not by the longer-time reorientation dynamics. As detailed in the SI, in contrast with our longer time τ_n values, the integrated reorientation times $\int_0^\infty C_n(t)\,dt$ considered in ref 7 include the initial librational decay. Librations make a growing contribution to the integrated times for increasing n; their amplitude's strong sensitivity to NQEs results in the observed increase with n of those times' quantum/classical acceleration (see the SI).

Turning to D_2O, Table 1 shows that reorientation times are not affected by NQEs. This does not imply that all D_2O motions are classical but rather that the competing NQEs on different degrees of freedom (*vide infra*) almost completely compensate each other; the D_2O rotational dynamics can then be correctly described by classical mechanics. (In contrast with the present q-TIP4P/F potential, typical force fields like SPC/E or TIP4P-2005 already include an effective description of NQEs for H_2O; thus, they cannot be adapted to D_2O by simply changing the hydrogen atoms' mass.)

Water reorientation has been argued[12,13] to proceed not by the traditional Debye diffusion mechanism but rather via sudden large angular jumps when an OH group trades H-bond acceptors (Figure 2a). As we will later pursue, these jump H-bond exchanges can be seen as a chemical reaction, breaking and making H-bonds.

Our quantum TRPMD simulations confirm that the jumps are still observed when NQEs are included (see the SI) and that their mechanism is very similar to that found in classical simulations. Figure 2b shows that the H_2O classical and quantum-mechanical jump angle distributions are practically identical. Because the jump amplitude $\Delta\theta$ is the angle formed by the three oxygen atoms depicted in Figure 2a,[12,13] their large effective mass leads to very limited quantum fluctuations.

Within the extended jump model[12,13] (EJM) description, the τ_n reorientation rate (inverse time) is the sum of the independent jump and frame reorientation rates. The reorientation times are thus determined by the jump time τ_0, defined as the inverse of the jump rate constant, the jump amplitude $\Delta\theta$, and the longer H-bond complex frame reorientation time between successive H-bond jumps. The latter is close to diffusive and is approximated by $1/[D_R^{frame} n(n+1)]$, where D_R^{frame} is the frame rotational diffusion constant. When the $P(\Delta\theta)$ jump angle distribution is explicitly considered, the EJM reorientation times are[13,19]

Table 1. Reorientation Times τ_n, Jump Time τ_0, Inverse of the Frame Rotational Diffusion Coefficient $1/D_R^{frame}$, and EJM Reorientation Times τ_n^{EJM} (eq 2), from Classical MD (cl) and TRPMD (qm) Simulations, Together with Their Ratios (all times in ps)

	H_2O			D_2O		
	cl	qm	qm/cl	cl	qm	qm/cl
τ_1	7.1(2)	6.1(1)	0.85(3)	8.0(3)	8.0(3)	1.00(5)
τ_2	3.7(1)	3.16(7)	0.86(4)	4.1(1)	4.12(7)	1.00(4)
τ_3	2.7(1)	2.26(4)	0.85(4)	2.9(1)	2.98(7)	1.02(5)
τ_0	4.4(1)	3.83(4)	0.87(3)	4.9(1)	4.87(5)	1.00(3)
$1/D_R^{frame}$	52(1)	45(1)	0.86(3)	56(2)	59(2)	1.04(5)
τ_1^{EJM}	7.1(1)	6.16(6)	0.87(2)	8.0(2)	8.0(1)	1.01(3)
τ_2^{EJM}	3.15(7)	2.73(3)	0.87(2)	3.50(7)	3.54(5)	1.01(3)
τ_3^{EJM}	2.09(4)	1.81(2)	0.87(2)	2.30(5)	2.34(4)	1.01(3)

DOI: 10.1021/acs.jpclett.7b00979
J. Phys. Chem. Lett. 2017, 8, 2602−2607

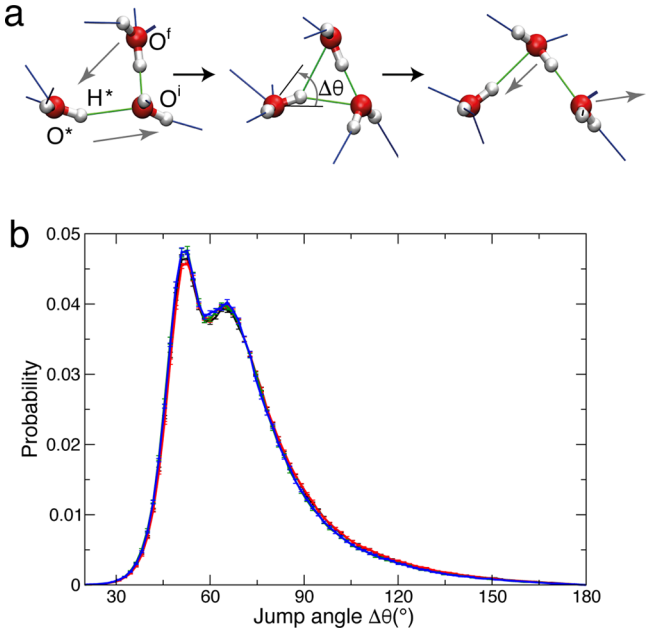

Figure 2. (a) Water jump mechanism[12,13] and (b) distributions of jump angles $\Delta\theta$ calculated from classical H_2O (black), quantum H_2O (red), classical D_2O (green), and quantum D_2O (blue) simulations; all distributions strongly overlap.

$$\frac{1}{\tau_n^{\mathrm{EJM}}} = \frac{1}{\tau_n^{\mathrm{jump}}} + \frac{1}{\tau_n^{\mathrm{frame}}} = \frac{1}{\tau_0}\left[1 - \frac{1}{2n+1}\int_0^{\pi} \mathrm{d}\Delta\theta\, P(\Delta\theta)\frac{\sin[(2n+1)\Delta\theta/2]}{\sin(\Delta\theta/2)}\right] + D_{\mathrm{R}}^{\mathrm{frame}} n(n+1) \quad (2)$$

We have computed the ingredients of the EJM as described in ref 13 using a Stable States approach to calculate τ_0 and a strict geometric H-bond definition (see the SI). As described in the SI, very similar results are obtained with the PAMM[20] probabilistic H-bond definition. In the quantum case, the ring-polymer centroids were used to calculate the jump rate constant.[21,22] The frame rotational diffusion constant $D_{\mathrm{R}}^{\mathrm{frame}}$ was determined from the first- and second-order reorientation times for an intact H-bonded pair of water molecules (see the SI). The resulting EJM reorientation times (eq 2) in Table 1 are seen to be in good agreement with the simulated τ_n values. This shows that the EJM initially suggested from analysis of classical MD[12,13] also provides a good description of water reorientation when NQEs are included. Accordingly, we can now use the EJM to determine the origin of the isotope and NQEs on water reorientation dynamics.

Table 1 shows that the acceleration of H_2O reorientation dynamics induced by quantum effects is essentially caused by acceleration in the jump dynamics (the frame reorientation is accelerated to the same extent as the jumps but remains much slower than the jumps in the classical and quantum descriptions). The jumps are the dominant reorientation pathway in both the classical and quantum cases, and the jump time τ_0 exhibits exactly the same acceleration as do the τ_n reorientation times.

We can therefore now focus on the origin of the NQE on the jump time. We immediately discard the possibility that a significant tunneling contribution could assist the water hydrogen atom's jump between the initial and final H-bond acceptors. In agreement with the conclusion of a preliminary study treating only the OH rotation quantum mechanically,[13] our quantum simulations show that the polymer beads' distribution at the jump transition state (TS) does not exhibit the bimodal behavior expected if tunneling were important (see the SI).

In order to analyze and understand the NQE for the jump kinetics, we require a comparable jump rate formulation for both the classical and quantum situations. In the classical case, viewing, as in the previous section, the jump as a chemical reaction in which the H-bond partners of the reorienting OH are exchanged leads[13] to the jump rate constant expression, here written in terms of its inverse, the jump time τ_0^{cl}

$$\tau_0^{\mathrm{cl}} = \frac{2\pi}{\omega^{\mathrm{cl}}} \exp(\Delta G_{\mathrm{cl}}^{\ddagger}/k_{\mathrm{b}}T) \quad (3)$$

Here ω^{cl} is the attempt frequency, that is, the frequency of the reaction coordinate for the reactant ($O^*H^*\cdots O^i$) configuration; $\Delta G_{\mathrm{cl}}^{\ddagger}$ is the activation free energy for the exchange, with the TS defined by the O*H* in-plane libration at the midpoint of the jump, with the two H-bonds of H* to O^i and O^f of equal length (see Figure 2a). $\Delta G_{\mathrm{cl}}^{\ddagger}$ can be decomposed into contributions from different coordinates in the passage from the reactant to the TS.[13,23] For the present q-TIP4P/F potential, the unstable reaction coordinate at the TS is the $O^iO^*O^f$ antisymmetric stretch compressing the new O^*O^f H-bond and expanding the old O^*O^i H-bond. (With the SPC/E potential and other classical potentials, at the TS, the in-plane O*H* libration has a double-well potential and the reaction coordinate is this libration.[13]) In the reactant, the reaction coordinate is the O^*O^f vibration (see the SI). All other coordinates, including, for example, the O*H* libration, the O*H* stretch and the solvent motions are stable, transverse coordinates both in the reactant and at the TS.

Turning to the quantum description, the H-bond exchange rate constant is not conveniently couched in such explicit ingredients. However, as argued in the SI, the reaction coordinate in the reactant (the O^*O^f vibration) and at the TS (the $O^iO^*O^f$ antisymmetric stretch) are well approximated as classical motions. In that case, we can employ an approach analogous to that used for proton transfer reactions[24,25] and write for the quantum case

$$\tau_0^{\mathrm{qu}} = \frac{2\pi}{\omega^{\mathrm{qu}}} \exp(\Delta G_{\mathrm{qu}}^{\ddagger}/k_{\mathrm{b}}T) \quad (4)$$

where the NQEs enter in the quantum free energy barrier $\Delta G_{\mathrm{qu}}^{\ddagger}$, which includes the difference of the ZPEs of the transverse coordinates in the reactant and at the TS.

To expose the NQE's major ingredients, we will later examine the ratio of eqs 4 and 3. First, we decompose the activation free energy in more detail. $\Delta G_{\mathrm{qu}}^{\ddagger}$ is the free energy change along the explicit H-bond-related reaction coordinate from reactant to TS, with all other, transverse, coordinates equilibrated to the reaction coordinate. (The actual dynamical path differs from this path, but this is irrelevant for the activation free energy calculation.) Because the classical and quantum mechanisms are the same, this is the free energy cost for the initial H-bond's elongation and for the final partner water molecule's approach to form the new H-bond.[13,23] Finally, the SI shows that it is a good approximation to treat this barrier simply as the sum of the two independent contributions of the O^*O^i and O^*O^f modes

DOI: 10.1021/acs.jpclett.7b00979
J. Phys. Chem. Lett. 2017, 8, 2602−2607

$$\Delta G^{\ddagger} \simeq \Delta G^{\ddagger}_{\mathrm{elong}} + \Delta G^{\dagger}_{\mathrm{compr}} \quad (5)$$

that is, to treat these modes as decoupled; here $\Delta G^{\ddagger}_{\mathrm{elong,compr}}$ are respectively the free energy costs for the elongation of the initial O^*O^i bond and for the compression of the O^*O^f distance.

Each term on the right-hand side of eq 5 corresponds to the free energy cost of bringing a pair of water molecules from their initial, reactant state, separation to their TS separation. These contributions can thus be straightforwardly determined from the potential of mean force (pmf) along the O−O distance $W(r)$, which is related to the rdf $g(r)$ between oxygen atoms, $W(r) = -k_B T \ln [g(r)]$. In the reactant state configuration, O^i lies in the first hydration shell of O*, so that the average O^*-O^i separation is the distance where the rdf exhibits its first peak r_{max1} (Figure 3). As for O^f, before the jump, it lies on average in the second shell[13] of O*, and the average O^*-O^f separation is therefore the radius at which the rdf exhibits its second peak, r_{max2} (Figure 3). At the jump TS, O^i and O^f are at the same distance from O*, which is that of the rdf's first minimum, r_{min} (Figure 3).

From this analysis, the free energy barrier in eq 5 can thus be approximated as

$$\Delta G^{\ddagger} \simeq [W(r_{\mathrm{min}}) - W(r_{\mathrm{max1}})] + [W(r_{\mathrm{min}}) - W(r_{\mathrm{max2}})] \quad (6)$$

as illustrated in Figure 3, and the classical and quantum jump times in eqs 3 and 4 can be estimated from the classical and quantum O−O rdfs $g^{\mathrm{cl,qu}}(r)$

$$\tau_0^{\mathrm{cl,qu}} \simeq \frac{2\pi}{\omega^{\mathrm{cl,qu}}} \frac{g^{\mathrm{cl,qu}}(r_{\mathrm{max1}})}{g^{\mathrm{cl,qu}}(r_{\mathrm{min}})} \frac{g^{\mathrm{cl,qu}}(r_{\mathrm{max2}})}{g^{\mathrm{cl,qu}}(r_{\mathrm{min}})} \quad (7)$$

We have computed the O−O rdf from both the classical and quantum simulations. As was originally found in pioneering quantum simulations of liquid water,[5,6] Figure 4 shows that while NQEs do not noticeably affect the D_2O rdf they do lead to a decrease in the H_2O rdf structure and thus to smaller pmf free energy barriers.

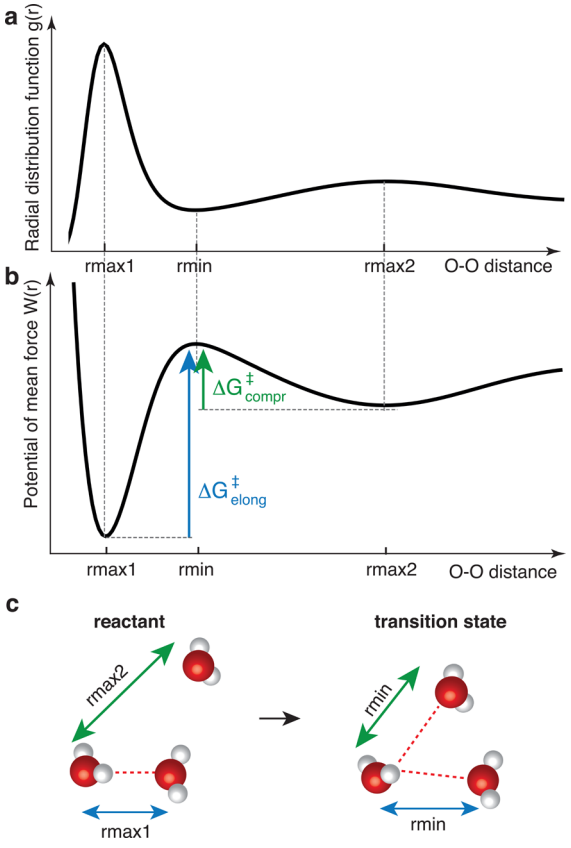

Figure 3. Schematic representation of the rdf $g(r)$ (a) and pmf $W(r)$ (b) along the O−O distance between two water oxygen atoms, together with the key changes in the O−O distances during the jump (c). The $\Delta G^{\ddagger}_{\mathrm{elong,compr}}$ free energy barriers respectively associated with the elongation of the initial O^*O^i H-bond (blue) and the compression of the O^*O^f distance to the new H-bond partner initially lying in the second hydration shell (green) are shown on the pmf. See the text.

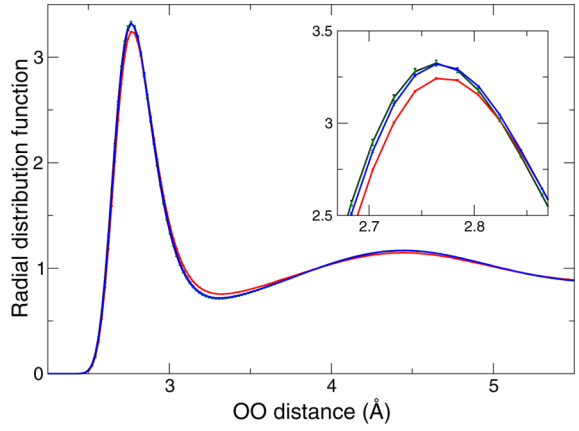

Figure 4. Rdfs in classical H_2O (black), quantum H_2O (red), classical D_2O (green), and quantum D_2O (blue), where the inset focuses on the first peak region. The error bars give the Student 95% confidence interval determined from the results obtained on the set of independent trajectories. The classical H_2O and D_2O distributions are almost superimposed, while for the quantum distributions, there is a smaller barrier for H_2O than for D_2O.

Recall from the discussion above eq 4 that the reaction coordinate comprises relative classical motions of O* and the oxygens of its initial and final H-bond partners; the quantum pmf therefore differs from the classical pmf because it includes ZPE contributions from all of the transverse coordinates, which vary with the O−O distance. Accordingly, we now explain the NQEs on the rdfs by considering the ZPEs of the three quantum H-bonding modes—the OH stretch and the two librational modes—and how they change when the H-bond is elongated. There are competing effects here: upon H-bond elongation, the H-bond acceptor attracts the H-bond donor hydrogen atom H* less strongly, so that with this now weaker H-bond H* becomes less delocalized along the stretch mode and the O*H* stretch ZPE increases. However, this weaker H-bond situation also decreases the restoring torque on the donor water molecule, which becomes more delocalized along the libration coordinate, whose ZPE thus decreases. Therefore, when the O−O distance increases, the stretch ZPE increases while the librational ZPE decreases. As was originally recognized in a nonreactive context[7,8] and has since been seen in several others,[26−28] the NQEs on stretch and librational modes thus partly compensate each other. The overall decrease in the structure of the H_2O rdf induced by NQEs (Figure 4) arises from the slightly dominant effect of the librational ZPE,

DOI: 10.1021/acs.jpclett.7b00979
J. Phys. Chem. Lett. 2017, 8, 2602−2607

which decreases the free energy barriers (see the SI). These competing quantum effects are thus essential to obtain a good description of the overall NQE on the dynamics. A prior study[29] of quantum effects on water jump dynamics, which also indicated that the jump mechanism remained a correct water reorientation description, made two important approximations that compromise this picture of competing effects: spherical Gaussian wavepackets having the same width along the OH stretch and OH libration modes and use of a water model with a harmonic OH stretch, in contrast with the present q-TIP4P/F model that accounts for this mode's anharmonicity.

Nuclear Quantum Effects and Isotope Effects. We now analyze the change in the jump times between two systems, conveniently labeled *a* and *b*, which differ either by their description of nuclear dynamics—quantum vs classical—or by their isotope—H_2O vs D_2O. Equations 3, 4, and (in particular) 7 show that the jump time can be described as the product of three terms, arising respectively from the frequency prefactor and from the change in the free energy costs to elongate the initial bond and compress the distance to the final acceptor, so that the ratio of *a* and *b* jump times has a corresponding product contribution with three ingredients:

$$\frac{\tau_0^a}{\tau_0^b} = \rho_\omega \rho_{\mathrm{elong}} \rho_{\mathrm{compr}}$$

$$\rho_\omega = \omega^b/\omega^a$$

$$\rho_{\mathrm{elong}} = e^{(\Delta G^{\ddagger a}_{\mathrm{elong}} - \Delta G^{\ddagger b}_{\mathrm{elong}})/k_bT} = \frac{g^a(r_{\mathrm{max1}})}{g^a(r_{\mathrm{min}})}\frac{g^b(r_{\mathrm{min}})}{g^b(r_{\mathrm{max1}})}$$

$$\rho_{\mathrm{compr}} = e^{(\Delta G^{\ddagger a}_{\mathrm{compr}} - \Delta G^{\ddagger b}_{\mathrm{compr}})/k_bT} = \frac{g^a(r_{\mathrm{max2}})}{g^a(r_{\mathrm{min}})}\frac{g^b(r_{\mathrm{min}})}{g^b(r_{\mathrm{max2}})} \quad (8)$$

Table 2 lists the contributions of each term in eq 8 and shows that it can quantitatively predict both the isotope and NQEs on the jump dynamics from the subtle changes in the rdf (Figure 4).

Table 2. Isotope and NQEs on the H-Bond Jump Times τ_0 Determined from Our Simulations and from Equation 8, Together with the Three Contributions in Equation 8 (See the SI)

		sim	eq 8	ρ_ω	ρ_{elong}	ρ_{compr}
τ_0^a/τ_0^c	H_2O	0.87	0.85	0.99	0.92	0.93
	D_2O	1.00	0.98	1.00	0.99	0.99
$\tau_0^{H_2O}/\tau_0^{D_2O}$	qm	0.79	0.82	0.95	0.93	0.93
	cl	0.90	0.94	0.95	0.99	0.99

We first analyze the NQE, that is, the ratio between the quantum and classical jump times. The ω attempt frequency depends on the reaction coordinate reduced mass and on the pmf curvature in the reactant region. Because NQEs do not change the reduced mass and induce very small changes in the pmf curvature (Figure 4), $\rho_\omega \simeq 1$. The key result shown by Table 2 is that the NQE acceleration in H_2O jump dynamics is due to the remaining two factors in the product, that is, comparable contributions from the easier elongation of the initial H-bond and from the more facile approach of the final H-bond partner. As described above, the lowering of these barriers for the O−O motions arises from the change in the OH libration ZPE, which is partly compensated by the change in the OH stretch ZPE. Although the jump reaction coordinate involving the heavy O atoms is essentially classical, the free energy cost of its rearrangements is affected by these NQE contributions transverse to the reaction coordinate because they change the interactions between the O atoms.

We now turn to the isotope effects, that is, application of eq 8 for the ratio between the H_2O and D_2O jump times. The ρ_ω ratio is $\sqrt{18/20}$ because the reaction coordinate involves the motion of water molecules and not solely their hydrogen/deuterium atoms. However, Table 2 reveals that the simple picture[30] assigning the isotope effect for assorted measures of water dynamics to this trivial mass effect in the present case considerably underestimates the quantum acceleration from D_2O to H_2O. Most of this acceleration is found to arise from the change in the rdf, which leads to a decrease in the H-bond exchange free energy barriers. (Strictly speaking, one should consider the rdfs and pmfs along the distance between the water molecules' centers of mass, but as shown in the SI, these are almost indistinguishable from their analogues along the O−O distance.) This acceleration from D_2O to H_2O in the NQE is due to the reduced ZPEs of the transverse coordinates in the heavier solvent.

Our results thus indicate that the mass of the isotope of the reorienting group is not the only factor that determines the isotope effect on the jump time and that the further contributions from H-bond expansion and compression in eq 8 can be important. This feature is illustrated by ultrafast spectroscopy experiments where the OD group of an HOD molecule immersed in H_2O was measured to reorient faster than the OH group of an HOD in D_2O (2.5 ± 0.2 vs 3.0 ± 0.3 ps[31]). This result may seem surprising because the lighter OH group might have been expected to reorient faster than the heavier OD. Although we did not explicitly consider these isotopic mixtures here, our results show that the influence of the isotopes present in the surrounding solvent makes a very important contribution to the dynamics because they determine the free energy cost of the new partner's approach (and the frame tumbling reorientation time[12,13]).

Our study has shown that the jump picture for water reorientation applies in the nuclear quantum mechanical description as well as in the classical regime. This has allowed us to identify the molecular factors explaining the nuclear quantum and isotope effects on water H-bond and reorientation dynamics. NQEs lead to a moderate water dynamics acceleration but do not affect the water reorientation mechanism, which mostly proceeds through large angular jumps, just as in the classical case. The changes in the H-bond jump dynamics are shown via a detailed jump perspective analysis to be semiquantitatively determined by the oxygen−oxygen rdf changes. Our study thus establishes a simple, robust relationship between the liquid structure and the dynamics of H-bond jumps, which are the elementary events governing water reorientation and, because each H-bond jump induces translation of the water molecules involved, translational dynamics.

■ ASSOCIATED CONTENT

Supporting Information

The Supporting Information is available free of charge on the ACS Publications website at DOI: 10.1021/acs.jpclett.7b00979.

Derivation of RPMD orientational time correlation functions and further discussion of the librational

DOI: 10.1021/acs.jpclett.7b00979
J. Phys. Chem. Lett. 2017, 8, 2602−2607

contribution to the integrated reorientation times, of the jump mechanism, of the PAMM H-bond analysis, of the correlated O^*-O^i and O^*-O^f distribution functions, and of the OH stretch and librational ZPEs (PDF)

AUTHOR INFORMATION

Corresponding Authors

*E-mail: david.wilkins@epfl.ch (D.M.W.).
*E-mail: david.manolopoulos@chem.ox.ac.uk (D.E.M.).
*E-mail: silvio.pipolo@univ-lille1.fr (S.P.).
*E-mail: damien.laage@ens.fr (D.L.).
*E-mail: james.hynes@colorado.edu (J.T.H.).

ORCID

Damien Laage: 0000-0001-5706-9939
James T. Hynes: 0000-0003-2683-0304

Present Address

§S.P.: Unité de Catalyze et Chimie du Solide, Université de Lille 1, 59655 Villeneuve d'Ascq, France.

Notes

The authors declare no competing financial interest.

ACKNOWLEDGMENTS

D.M.W. thanks M. Rossi and M. Ceriotti for helpful discussions and P. Gasparotto for advice on the PAMM algorithm. Financial support from a CNRS − Royal Society international collaborative grant (D.E.M., D.L., and J.T.H.), the Agence Nationale de la Recherche (Grant ANR-11-BSV5-027 to D.L.), and NSF (Grant CHE-1112564 to J.T.H.) is acknowledged. D.L. thanks D.E.M. and his group for their hospitality at Oxford where this work was completed.

REFERENCES

(1) Ball, P. Water as an Active Constituent in Cell Biology. *Chem. Rev.* **2008**, *108*, 74−108.
(2) Laage, D.; Stirnemann, G.; Sterpone, F.; Rey, R.; Hynes, J. T. Reorientation and Allied Dynamics in Water and Aqueous Solutions. *Annu. Rev. Phys. Chem.* **2011**, *62*, 395−416.
(3) Levy, Y.; Onuchic, J. N. Water mediation in protein folding and molecular recognition. *Annu. Rev. Biophys. Biomol. Struct.* **2006**, *35*, 389−415.
(4) Berkelbach, T. C.; Tuckerman, M. E.; Lee, H.-S. Concerted Hydrogen-Bond Dynamics in the Transport Mechanism of the Hydrated Proton: A First-Principles Molecular Dynamics Study. *Phys. Rev. Lett.* **2009**, *103*, 238302.
(5) Kuharski, R. A.; Rossky, P. J. A quantum mechanical study of structure in liquid H_2O and D_2O. *J. Chem. Phys.* **1985**, *82*, 5164−5177.
(6) Wallqvist, A.; Berne, B. J. Path-integral simulation of pure water. *Chem. Phys. Lett.* **1985**, *117*, 214−219.
(7) Habershon, S.; Markland, T. E.; Manolopoulos, D. E. Competing quantum effects in the dynamics of a flexible water model. *J. Chem. Phys.* **2009**, *131*, 024501.
(8) Li, X.-Z.; Walker, B.; Michaelides, A. Quantum nature of the hydrogen bond. *Proc. Natl. Acad. Sci. U. S. A.* **2011**, *108*, 6369−6373.
(9) Miller, T. F.; Manolopoulos, D. E. Quantum diffusion in liquid water from ring polymer molecular dynamics. *J. Chem. Phys.* **2005**, *123*, 154504.
(10) Paesani, F.; Iuchi, S.; Voth, G. A. Quantum effects in liquid water from an ab initio-based polarizable force field. *J. Chem. Phys.* **2007**, *127*, 074506.
(11) Paesani, F.; Yoo, S.; Bakker, H. J.; Xantheas, S. S. Nuclear Quantum Effects in the Reorientation of Water. *J. Phys. Chem. Lett.* **2010**, *1*, 2316.
(12) Laage, D.; Hynes, J. T. A Molecular Jump Mechanism of Water Reorientation. *Science* **2006**, *311*, 832−835.
(13) Laage, D.; Hynes, J. T. On the Molecular Mechanism of Water Reorientation. *J. Phys. Chem. B* **2008**, *112*, 14230−14242.
(14) Ludwig, R. The mechanism of the molecular reorientation in water. *ChemPhysChem* **2007**, *8*, 44−46.
(15) Rossi, M.; Ceriotti, M.; Manolopoulos, D. E. How to remove the spurious resonances from ring polymer molecular dynamics. *J. Chem. Phys.* **2014**, *140*, 234116.
(16) Medders, G. R.; Babin, V.; Paesani, F. Development of a First-Principles Water Potential with Flexible Monomers. III. Liquid Phase Properties. *J. Chem. Theory Comput.* **2014**, *10*, 2906−2910.
(17) Kell, G. S. Precise representation of volume properties of water at one atmosphere. *J. Chem. Eng. Data* **1967**, *12*, 66−69.
(18) Fogarty, A. C.; Duboué-Dijon, E.; Sterpone, F.; Hynes, J. T.; Laage, D. *Chem. Soc. Rev.* **2013**, *42*, 5672−5683.
(19) Boisson, J.; Stirnemann, G.; Laage, D.; Hynes, J. T. Water reorientation dynamics in the first hydration shells of F^- and I^-. *Phys. Chem. Chem. Phys.* **2011**, *13*, 19895−19901.
(20) Gasparotto, P.; Ceriotti, M. Recognizing molecular patterns by machine learning: An agnostic structural definition of the hydrogen bond. *J. Chem. Phys.* **2014**, *141*, 174110.
(21) Craig, I. R.; Manolopoulos, D. E. Chemical reaction rates from ring polymer molecular dynamics. *J. Chem. Phys.* **2005**, *122*, 084106.
(22) Craig, I. R.; Manolopoulos, D. E. A refined ring polymer molecular dynamics theory of chemical reaction rates. *J. Chem. Phys.* **2005**, *123*, 034102.
(23) Stirnemann, G.; Laage, D. Direct Evidence of Angular Jumps During Water Reorientation Through Two-Dimensional Infrared Anisotropy. *J. Phys. Chem. Lett.* **2010**, *1*, 1511−1516.
(24) Kiefer, P. M.; Hynes, J. T. Nonlinear Free Energy Relations for Adiabatic Proton Transfer Reactions in a Polar Environment. I. Fixed Proton DonorAcceptor Separation. *J. Phys. Chem. A* **2002**, *106*, 1834−1849.
(25) Kiefer, P. M.; Hynes, J. T. Nonlinear Free Energy Relations for Adiabatic Proton Transfer Reactions in a Polar Environment. II. Inclusion of the Hydrogen Bond Vibration. *J. Phys. Chem. A* **2002**, *106*, 1850−1861.
(26) Markland, T. E.; Berne, B. J. Unraveling quantum mechanical effects in water using isotopic fractionation. *Proc. Natl. Acad. Sci. U. S. A.* **2012**, *109*, 7988−7991.
(27) Liu, J.; Andino, R. S.; Miller, C. M.; Chen, X.; Wilkins, D. M.; Ceriotti, M.; Manolopoulos, D. E. A Surface-Specific Isotope Effect in Mixtures of Light and Heavy Water. *J. Phys. Chem. C* **2013**, *117*, 2944−2951.
(28) Wilkins, D. M.; Manolopoulos, D. E.; Dang, L. X. Nuclear quantum effects in water exchange around lithium and fluoride ions. *J. Chem. Phys.* **2015**, *142*, 064509.
(29) Ono, J.; Hyeon-Deuk, K.; Ando, K. Semiquantal molecular dynamics simulations of hydrogen-bond dynamics in liquid water using spherical Gaussian wave packets. *Int. J. Quantum Chem.* **2013**, *113*, 356−365.
(30) Ceriotti, M.; Fang, W.; Kusalik, P. G.; McKenzie, R. H.; Michaelides, A.; Morales, M. A.; Markland, T. E. Nuclear Quantum Effects in Water and Aqueous Systems: Experiment, Theory, and Current Challenges. *Chem. Rev.* **2016**, *116*, 7529−7550.
(31) Bakker, H. J.; Rezus, Y. L. A.; Timmer, R. L. A. Molecular reorientation of liquid water studied with femtosecond midinfrared spectroscopy. *J. Phys. Chem. A* **2008**, *112*, 11523−11534.

DOI: 10.1021/acs.jpclett.7b00979
J. Phys. Chem. Lett. 2017, 8, 2602−2607